Journal Pre-proof

An impedimetric biosensor system based on disposable graphite paper electrodes: Detection of ST2 as a potential biomarker for cardiovascular disease in human serum

Burçak DEMİRBAKAN, Mustafa Kemal SEZGİNTÜRK

PII: S0003-2670(20)31188-0

DOI: https://doi.org/10.1016/j.aca.2020.12.001

Reference: ACA 238126

To appear in: *Analytica Chimica Acta*

Received Date: 17 September 2020

Revised Date: 20 November 2020

Accepted Date: 1 December 2020

Please cite this article as: B. DEMİRBAKAN, M. Kemal SEZGİNTÜRK, An impedimetric biosensor system based on disposable graphite paper electrodes: Detection of ST2 as a potential biomarker for cardiovascular disease in human serum, *Analytica Chimica Acta*, https://doi.org/10.1016/j.aca.2020.12.001.

CREDIT AUTHOR STATEMENT

Title

An impedimetric biosensor system based on disposable graphite paper electrodes: Detection of ST2 as a potential biomarker for cardiovascular disease in human serum

Corresponding Author : Assist. Prof. Dr. Burçak DEMİRBAKAN

Investigation, Experimental Section, Writing- Reviewing and Editing

Author : Mustafa Kemal SEZGİNTÜRK

Reviewing and Editing

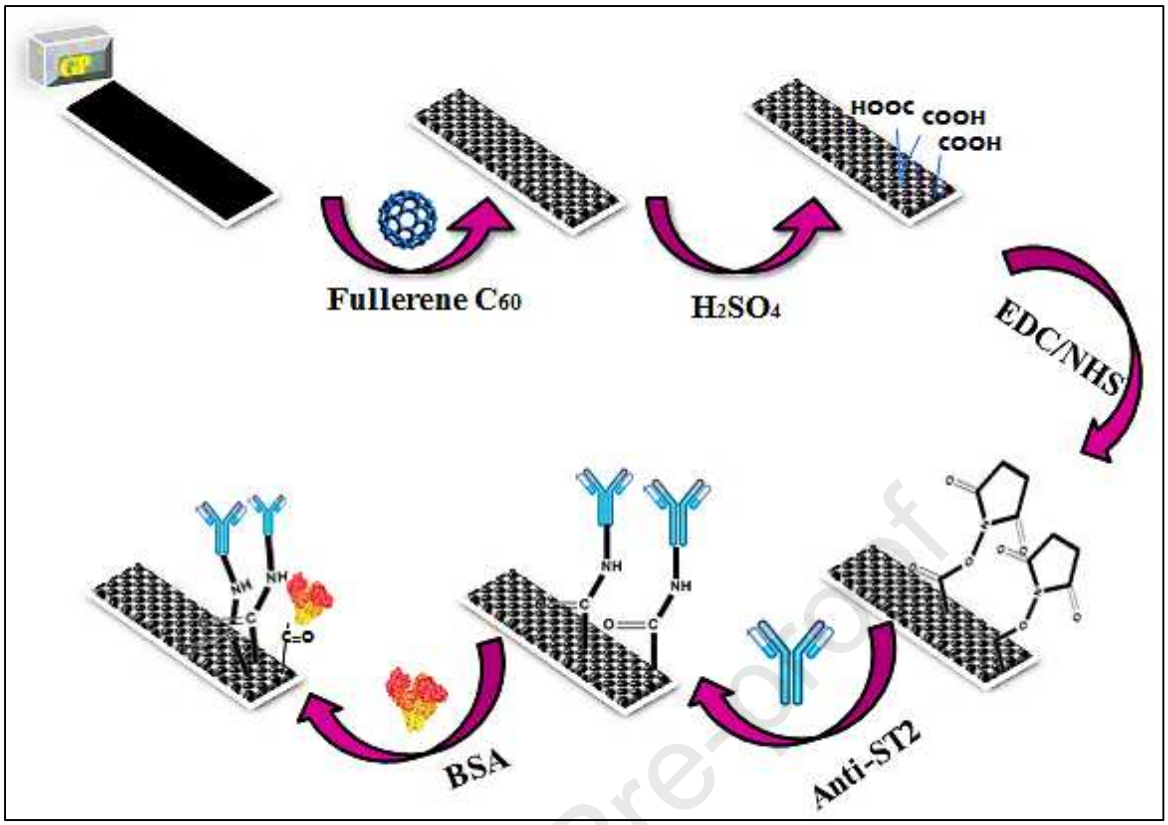

An impedimetric biosensor system based on disposable graphite paper electrodes: Detection of ST2 as a potential biomarker for cardiovascular disease in human serum

Burçak DEMİRBAKAN[a*], Mustafa Kemal SEZGİNTÜRK[a]

[a]Çanakkale Onsekiz Mart University, Faculty of Engineering, Bioengineering Department, Çanakkale-TURKEY

[a*]Corresponding Author:

e-mail: burcakdemirbakan@comu.edu.tr

Tel:+90 537 895 70 51

[a]Author :

e-mail: msezginturk@comu.edu.tr

ABSTRACT

In present study, we developed a highly sensitive, electrochemical immunosensor based on fullerene C_{60}-modified disposable graphite paper (GP) electrode for determination of Suppression of Tumorigenicity 2 (ST2) in human serum. The synthesis of the ST2 immunosensor was monitored with electrochemical impedance spectroscopy (EIS), cyclic voltammetry (CV) techniques and single frequency impedance (SFI) technique which is utilized for the specific interaction between anti-ST2 and ST2 antigen. Moreover, the morphological alteration of each GP surface was examined by scanning electron microscopy (SEM), SEM-energy dispersive X-ray spectroscopy (EDX) and atomic force microscopy (AFM). All parameters such as fullerene C_{60} concentration, antibody concentration and antibody incubation time were optimized. Analytical characteristics such as linear determination range, repeatability, reproducibility, regeneration and surface coverage were determined for the immunosensor. The ST2 electrochemical immunosensor had excellent repeatability, reproducibility and a wide detection range (from 0.1 fg mL^{-1} to 100 fg mL^{-1}). The proposed immunosensor also had low limit of detection (LOD) and limit of quantification (LOQ) values of 0.124 fg mL^{-1} and 0.414 fg mL^{-1}, respectively. The proposed immunosensor was applied to real samples to test applicability in clinical practice.

Keywords: Graphite paper (GP), Suppression of Tumorigenicity 2 (ST2), biosensor, cardiovascular disease.

1. Introduction

ST2 is a member of an interleukin-1 receptor family with trans-membrane (ST2L) and soluble (sST2) isoforms. ST2L is a membrane-bound isoform with 3 extracellular IgG domains, a single trans-membrane region, and an intracellular domain. sST2 is devoid of trans-membrane and intracellular domains [1]. ST2L and sST2 are produced by alternating promoter chains [2]. Although interleukin-33 is known before, the pathophysiological role of ST2L is not fully understood. It is defined as a functional ligand of ST2L [3]. It is claimed that interleukin-33/ST2L signaling functions are an important cardioprotective mechanism protecting the myocardium under mechanical overload, in addition to functions in several tissues [4]. Sepsis and consecutive multiorgan failure/dysfunction syndrome (MOF/MODS) are associated with poor symptoms and septic shock is the most common cause of death in intensive care units [5]. The immunological cascade of the sepsis response leads to increased T-cell apoptosis, lymphopenia, and altered T-lymphocyte subpopulations [6]. The specific type of immune response is determined by the differentiation of T helper (Th0) cells to Th1 or Th2 cells. Furthermore, Th2 antibody-mediated immune responses appear dominant in sepsis [7, 8]. In addition, ST2 proteins called T1, Fit-1, and DER4 are new Th2-specific products. Three different types of gene products belonging to ST2 are cloned as soluble ST2 (ST2), trans-membrane receptor form (ST2L) and variant form (ST2 V) of ST2 [9, 10, 11]. ST2 encodes a rare receptor of the Ig superfamily and the ST2 gene is firmly bound to genes encoding IL-1 receptor type I and type II on the human chromosome [12, 2, 13]. According to the Human Gene Nomenclature Database, interleukin-1 receptor-like-1 (IL1R1) represents soluble ST2. IL1RL1-a is soluble ST2 receptor and IL1R1-b is ST2L [14]. ST2 genes are preferably expressed on activated Th2 cells instead of Th1 cells and play an important role in Th2 effector functions [15] characterized by elevated expression of IL-4, IL-5 and IL-13 cytokines [15, 16, 17]. The serum ST2 protein concentrations increase in fibrosis, various autoimmune diseases, and idiopathic pulmonary disease [18, 19].

ST2 is a very important potential biomarker for the early diagnosis of cardiovascular diseases and it provides prognostic information in low-risk community-based populations[20]. Moreover, sST2 has determined in the serum of patients immediately after acute myocardial infarction. The situation suggests that ST2 is rapidly and transiently induced in humans and that soluble ST2 is chronically increased in patients with heart failure [21]. Also, higher sST2 levels are also associated with an increased risk of unfavorable left ventricular remodeling [22]. Additionally; ST2 is predicted to function as a decoy receptor counteracting the positive

effects of interleukin-33 binding to the membrane bound receptor isoform of ST2L [23]. All these critical roles of ST2 clearly reveal the need for a practical, economical and most importantly sensitive biosensor that can determine its level in serum for early detection.

Cardiovascular diseases (CVD) are one of the main causes of death globally. These diseases include non-rhythmic heart, failure of blood vessels, acute myocardial infarction, coronary failure and many other cardiovascular diseases [24]. The World Health Organization (WHO) reported that the deaths of 20 million people (approximately, 31% of all global deaths) were related to cardiovascular disease in 2015 [25]. CVD is generally caused by malnutrition, smoking habits, drug habits, alcohol use, excessive stress, and the lifestyle of the person [26]. Biosensor systems developed for early detection of these diseases play a critical role with many different effects. The early detection of CVD is crucial for clinical diagnosis of people with this disease or who are at risk.

Graphite paper electrode has the excellent flexibility and roughness surface, electrochemical energy conversion and storage devices, such as redox, are very useful as they enable a wider use of batteries [27], microbial fuel cells [28] and super capacitor. Moreover, this excellent material has very advantages for developing immunosensor systems such as low-cost, high electrical conductivity and practical immobilization methods [29, 30].

Fullerenes have unique electronic and chemical properties [31]. Molecular engineering has enormous potential power for new molecular materials and supramolecular chemistry [32]. Many examples of fullerene derivatives used in medical applications or nanotechnology have been synthesized for a long time with promising developments. Fullerene C_{60} has a broad range of charming properties such as super conductivity, mechanical strength, thermal stability etc. But application of such enormous properties of fullerene C_{60} has been majorly frustrated owing to the inadequate workability of fullerene C_{60} [33, 34, 35]. In recent years, there has been an increase in the development of fullerene C_{60} modified biosensors due to these advantageous properties. However, in many studies, it is seen that biosensors designed as fullerene C_{60} modified have a detection range that can measure at high concentration concentrations (at uM and nM levels, e.g) [36,37,38]. This is a problem in biosensor systems developed for biomarkers that can be detected at lower concentrations. A solution to this problem would be to design a fullerene C_{60}-modified biosensor capable of measuring at lower concentrations.

In this study, a biosensor system with disposable electrodes and several electrochemical techniques was designed to determine ST2 which is important as a potential biomarker for early detection of cardiovascular diseases. This novel electrochemical biosensor system developed with GP electrodes represents a practical, low-cost and sensitive method of analysis to determine ST2, using the EIS technique for the first time. Electrochemical impedance spectroscopy, cyclic voltammetry, square wave voltammetry and single frequency technique were utilized for immobilization, optimization and characterization studies when designing the biosensor. SEM was used to monitor the morphological changes of the surface during the immobilization step. The clinical potential of the proposed immunosensor was investigated by analyzing real serum samples with standard addition method. It was observed that the biosensor system developed for detection of cardiovascular diseases has very high sensitivity, excellent reproducibility and reusability capacity, long shelf life and high sensitivity for the analysis of serum samples. The analytical comparison of the designed biosensor with the various ST2 sensors reported in the literature is given in Table 1.

Table 1

2. Experimental

2.1. Materials

All chemicals (Fullerene C_{60}, N-(3-Dimethylaminopropyl)-N′-ethylcarbodiimide (EDC), N-hydroxysuccinimide (NHS), sulfuric acid (H_2SO_4, 95-98%), toluene (99.8%)), and biorecognition materials (ST2 antibody, ST2 antigen and BSA (bovine serum albumin) protein) were purchased from Sigma-Aldrich (St. Louis, M.O., USA). Graphite paper (GP) sheets (thickness: 0.3±0.01 mm, size: 210 mm x 210 mm, 3 mΩ/ cm^2) were purchased from Xiamen Tob New Energy Technology (Co. Ltd, Fujian, China). Reference electrode and counter electrode were purchased from BASi (West Lafayette, IN, USA). The whole proteins were formed by using a phosphate buffer (50 mM, pH 7.0) and kept at -20 °C until use. Also, 5 mM $[Fe(CN)_6]^4$/5 mM $[Fe(CN)_6]^3$ (1:1), which is a redox probe solution containing 0.1 M KCl, was prepared with ultra-pure water. In this study a three-electrode system with Ag/AgCl (saturated with KCl) as a reference electrode, a platinum wire as a counter electrode and disposable GP electrode as a working electrode (5 mm x 20 mm, 3 mΩ/ cm^2) were used. Clinical human serum samples were obtained from Çanakkale Onsekiz Mart University Hospital.

2.2. Instruments

All electrochemical impedance, cyclic voltammetry and square wave voltammetry analyses were performed with Gamry Potentiostat/Galvanostat (Reference 600, Gamry Instruments, Warminster, PA, USA) connected with a computer via EChem Analyst software throughout the entire study. PURELAB flex 3 & 4 Ultrapure Water Purification System (ELGA LC 134 model) was used for ultra-pure water during all preparation stages of the proposed immunosensor. The surface morphologies of GP electrodes were examined through monitoring with a thermal field emission scanning electron microscope (JEOL JSM-7100F model). EDX spectra were measured using the detector in the Oxford Instrument X-Max brand-model. AFM images were measured using WITEC ALPHA 3100R model. The SEM, EDX and AFM measurements were carried out at the Science and Technology Application and Research Center of Çanakkale Onsekiz Mart University (ÇOBİLTUM). To obtain the SEM images, 5 kV was used as acceleration voltage.

2.3. Construction of the proposed immunosensor

The proposed immunosensor was fabricated by using disposable GP electrodes. First of all, the electrodes were cleaned in ethanol and ultra-pure water (18.2 MΩ deionized) with the help of an ultrasonic bath for 5 min, respectively. Thereafter, the GP electrodes were coated with fullerene C_{60} solution (in toluene) and carefully dried with pure argon gas. To disturb carboxyl groups on the electrode surface, it was incubated with H_2SO_4 solution (0.018 M, v/v) overnight in darkness. After the H_2SO_4 process, the EIS and CV measurements of the GP electrodes were taken and they were incubated in EDC/NHS (0.4 mM; 0.1 mM) which was prepared in phosphate buffer (pH 7.0) for 1 h. In the next step, anti-ST2 antibodies were immobilized onto the GP electrode surface. For this process, the electrodes were immersed in anti-ST2 solutions at room temperature for 60 min. Then, BSA protein (0.5 %, w/v) was utilized as a blocking agent in order to inhibit non-specific interactions on the GP electrode surface. In the last step, the proposed immunosensor was prepared to detect ST2 antigen. After all immobilization steps of the proposed immunosensor, GP electrodes were washed with ultra-pure water and dried with argon stream. Meanwhile, all electrochemical processes were completed at 25 °C. The construction steps of the proposed immunosensor are presented in Scheme 1.

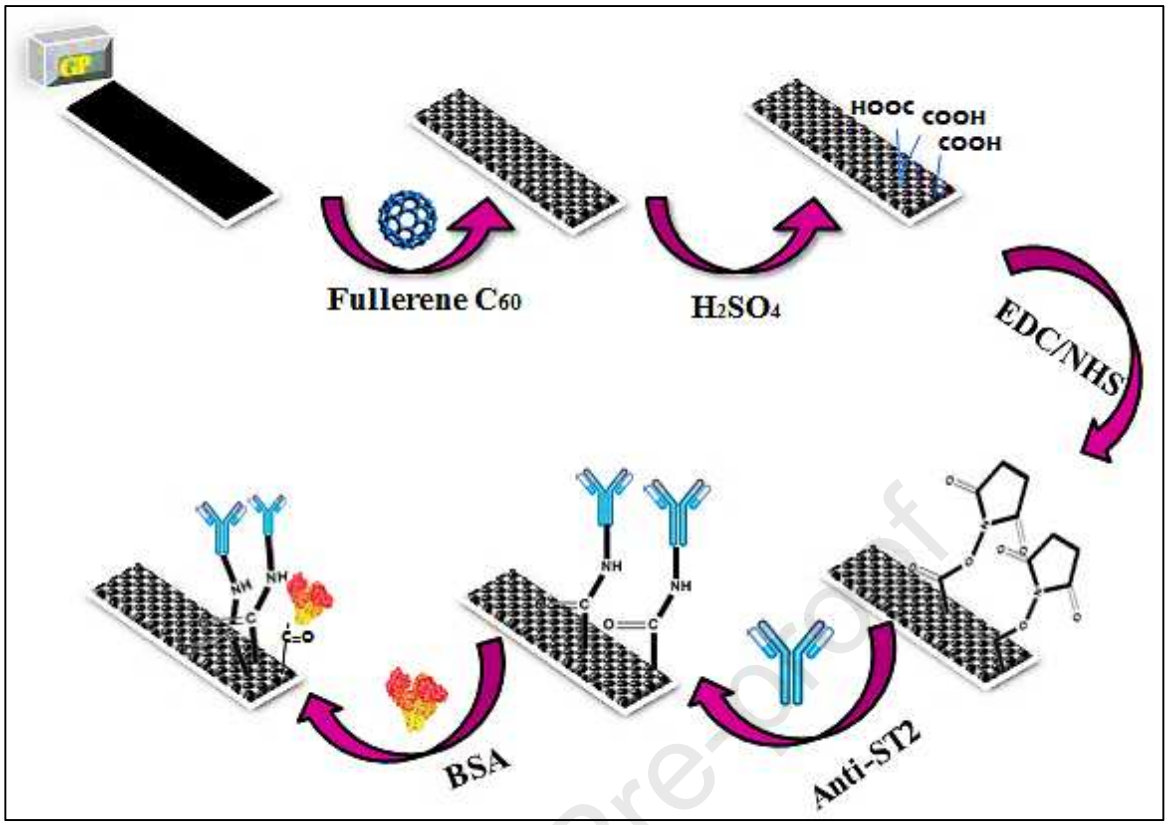

Scheme 1. The immobilization scheme of the ST2 immunosensor.

2.4. Principle of measurement for the proposed immunosensor

The electrochemical impedance spectroscopy and the cyclic voltammetry were used for all immobilization steps of the proposed immunosensor. The CV measurements were carried out in a potential range (-0.5 V to 1 V; step size: 10 mV; scan rate: 100 mVs^{-1}) with KCl (0.1 M) and $K_3[Fe(CN)_6]/K_4[Fe(CN)_6]$ (5mM, 1:1) solution as a redox probe. Electrochemical impedance measurements were carried out at 10.000 Hz – 0.05 Hz frequency range. Square wave voltammetry measurements were performed in the potential range (-0.2 V to 0.7 V; frequency: 25 Hz; pulse size: 25 mV; equil. time: 2 s).

2.5. Real serum analysis of the proposed immunosensor

The proposed immunosensor was applied to real human serum samples. This study was performed by preparing three GP electrodes for different ST2 concentrations (5 fg mL^{-1} and 50 fg mL^{-1}). These GP electrodes were prepared from the serum samples of 5 different individuals and the study was carried out by the standard addition method. The standard addition method was performed by making necessary dilution procedures (1000-fold dilution) [39] with phosphate buffer (0.05 M, pH 7.4) in accordance with the determination range of

ST2 in human serum. The relative standard deviation (RSD) and the recovery values were calculated using equations obtained from the calibration graph of the immunosensor (Table 2).

Table 2

3. Discussion and Results

3.1. Direct electrochemistry of ST2 immunosensor on modified GPs

Electrochemical impedance spectroscopy and cyclic voltammetry are efficient techniques to research the immobilization on electrochemical immunosensors. The EIS technique is utilized with a Randless equivalent circuit which involves the charge transfer resistance (Rct), the solution resistance (Rs), the constant phase element (CPE) and Warburg impedance (W). The diameter of the semicircle of the EIS data corresponds to the Rct value in the Nyquist plot [40]. First, the immobilization steps of the ST2 immunosensor were examined with the help of the EIS technique. Fullerene C_{60} nanomaterial was found to form a more stable carbon surface in the immobilization process of the proposed immunosensor. This nanomaterial was formed by a perfect configuration of carbon atoms which aided in creating a more homogeneous surface. The fullerene C_{60} should be in solution for chemical modification [41]. Therefore, it was solubilized in pure toluene [42] and incubated for the immobilization of the carbon atoms. The bioelectrochemical redox behavior of the fullerene C_{60} was monitored as a signal increase in Fig.1A. After the cleaned electrode surface was coated with fullerene C_{60}, the Rct value of the EIS signal clearly increased (Fig.1B). Then, the GP electrodes were incubated to quantitatively increase the carboxyl groups on the surface with H_2SO_4 solution overnight. This incubation caused a decrease in the Rct value. This may be due to the increase in diffusion resulting from the homogeneous layer coated with fullerene C_{60} being degraded by acid treatment and the increase in the porous structure of the electrode surface. The EDC/NHS couple which is a cross-linker was used to activate carboxyl groups on the GP surface. After this reaction, the Rct value also decreased after activation with EDC / NHS due to neutralization of the negative charge of the surface-bound -COOH groups. Moreover, the EDC/NHS provided surface immobilization of the anti-ST2 thanks to crosslinking between carboxylic acid groups of H_2SO_4. After anti-ST2 immobilization, the EIS signal increased gradually. The BSA blockage agent (0.5%, w/v) was used to inhibit non-specific interactions in the last step of immobilization. After the BSA incubation, the EIS signal significantly increased due to decreasing electron transfer on the insulating electrode surface.

In addition to the EIS technique, measurements were taken with the CV technique to support the accuracy of the results. As seen in Fig.1C, after the cleaning procedure, the bare GP electrode had regular peak currents (Cathodic peak current=846.5 μA, Anodic peak current =881.7 μA). When the surface of the GP electrode was further coated with fullerene C_{60} nanomaterial, the peak potentials of the GP/Fullerene C_{60} decreased (cathodic peak current=358.4 μA, anodic peak current =336.5 μA), obviously. The reason for this difference is that the electrode surface layer is insulated with the fullerene C_{60}. Immediately after the acid treatment, the peak currents were seen to be slightly higher than fullerene C_{60} from the previous step (cathodic peak current=479.4 μA, anodic peak current =480.5 μA) and they were further increased by EDC/NHS treatment (cathodic peak current=522 μA, anodic peak current =597.7 μA). When the antibody immobilization step is carried out, the cathodic peak current as an indicator of insulation was calculated as 519.3 μA and the anodic peak current was 554.2 μA. In the final step of the immobilization, the peak currents decreased in the same way after BSA protein was used to block non-specific sites (cathodic peak current=453 μA, anodic peak current =454.7 μA) (Fig.1C).

Figure 1

3.2. Morphological Characterization of ST2 immunosensor

SEM images for each of the immobilization steps were taken to examine the morphological changes occurring on the surface. The SEM images of ST2 biosensor are given in Fig.2. The first image belongs to the clean electrode surface (Fig.2A). There is no heterogeneous appearance on the surface where immobilization process was not generated. Fig .2B shows the SEM image after the surface was modified with fullerene C_{60}. In this image, the presence of fullerene C_{60} molecules is very clear. This image, reminiscent of a cobweb woven with nanowires, proves that the fullerene C_{60} is adsorbed onto the surface. Fig.2C presents the electrode surface after incubation with H_2SO_4 overnight. In Fig.2C, a morphological image similar to the structures dispersed on the electrode surface was observed after acid treatment. The SEM image in Fig.2D belongs to the EDC/NHS crosslinker. This image also has a completely different morphology from the previous surface. The reason for this morphological change is thought to be the carboxyl groups activated by EDC/NHS. Fig.2E illustrates the electrode surface after anti-ST2 immobilization. It is thought that the folded structures, which appear quite dense on the surface, are formed after the immobilization of the antibody. The image seen in Fig.2F belongs to the BSA blocking step. The structures

appearing among the nanowire-like structures were observed on the surface after BSA treatment. Finally, Fig.2G presents the electrode surface image belonging to the ST2 biomarker. This image, which is reminiscent of a flowering branch, was observed after the ST2 protein was incubated on the electrode surface.

Further characterizations of bare GP electrode surface and GP electrode surface were performed with SEM-EDX with elemental mapping measurements (Fig. 2H and 2J).. As illustrated in Fig. 2K, after the ST2 immobilization, GP surface had carbon (C), oxygen (O) and nitrogen (N) elements. These results were consistent with the literature. The carbon element (red) was observed in Fig. 2I and the carbon element of carboxyl groups was onto the graphite paper surface. The ratio of carbon element in EDX analysis was 87.4 %. Additionally, the oxygen (blue) and nitrogen (green) were also observed in Fig.2I and the ratio of oxygen and nitrogen elements in EDX analysis was 10.2 % and 2.4 %, respectively. It is obvious that a layer of successfully immobilization was assembled onto the GP surface.

Morphological characterization of the ST2 immunosensor was also confirmed by AFM analyses. Fig.S2 illustrates the surface images of GP electrodes after every immobilization stage. It can be seen from Fig.S2A, GP electrode surface was smooth. AFM image (Fig. 2A) also supported the SEM image. The surface roughness value was measured as 637.5 nm after fullerene C_{60} modification. After H_2SO_4 immobilization, the morphology of the fullerene C_{60} modified GP electrode was diversified. As observed in Fig. S3E, anti-ST2 antibodies were clearly visible on the GP electrode surface. The surface roughness of anti-ST2 attached GP electrode increased to 531.1 nm (Fig. S3E). After elimination of free epoxy groups with BSA coupling agent, the surface roughness was decreased (Fig. S3F) and the surface roughness of GP/fullerene C_{60} /H_2SO_4/EDC-NHS/anti-ST2/BSA electrode was 462.3 nm. Fig. S3G demonstrated the successful immobilization of ST2 antigen on the GP surface. The surface roughness of GP/fullerene C_{60} /H_2SO_4/EDC-NHS/anti-ST2/BSA/ST2 electrode was 15.16 nm (Fig. S3G). This increase in surface roughness value demonstrated that the ST2 antigen was successfully immobilized on the GP surface. The results of SEM and AFM characterizations were in accordance with electrochemical characterization techniques.

Figure 2

3.3. Optimization Steps for ST2 immunosensor

3.3.1. Optimization studies of fullerene C_{60} nanomaterial

The optimization studies of the proposed immunosensor were carried out for each parameter. In order to investigate the effect of the amount of fullerene C_{60} on the biosensor, all other parameters were kept constant and the biosensors were prepared with different concentrations of fullerene C_{60}. First, the amount of fullerene C_{60} was optimized by using three different concentration values (0.2 mg mL^{-1}, 0.4 mg mL^{-1} and 0.8 mg mL^{-1}) prepared in toluene solution. The biosensors were prepared with these concentrations of fullerene C_{60} and standard graphics for the ST2 biosensor were obtained. Fig.S1 displays the optimization result for the amount of fullerene C_{60}. First of all, a biosensor was prepared by using 0.2 mg fullerene C_{60}. Then, the amount of fullerene C_{60} was increased and the biosensor was prepared by using 0.4 mg fullerene C_{60}. When the graphs in Fig.S1A were examined, it is seen that higher signals were obtained by increasing the concentration of fullerene C_{60} (from 0.2 mg/mL to 0.4 mg/mL). Accordingly, the concentration of fullerene C_{60} was further increased (0.8 mg/mL). However, by using more concentrated fullerene C_{60}, the homogenous layer could not be formed on the surface and adsorption could not be achieved. Thus, the EIS signals decreased. For this reason, 0.4 mg mL^{-1} was chosen as the optimum concentration of fullerene C_{60}. The standard graphs for this optimization step are shown in Fig.S1A.

When developing a biosensor, it is necessary to determine the optimum incubation times for the agents used for the surface modification because these periods directly affect the immobilization process. In this study, the electrodes were incubated with fullerene C_{60} for different periods (30 min, 60 min and 120 min). Then, the EIS and the CV measurements were performed. It was observed that incubation of the GP electrodes with fullerene C_{60} nanomaterial for 30 min was not sufficient for a good immobilization process. Fullerene C_{60} nanomaterial which is holding onto the surface by adsorption, could not form a suitable layer for immobilization for 30 min. Put it differently, it could not form enough carboxyl groups on the surface. Also, the incubation period of 120 min caused some deterioration. For this reason, the fullerene, which remained on the electrode surface for too long and negatively affected the activity of carboxyl groups. Based on these results, the incubation period of fullerene C_{60} nanomaterial was chosen as 60 min. The standard graphs belonging to the incubation periods of fullerene C_{60} are shown in Fig.S1B.

3.3.2. Determination of optimum H_2SO_4 acid concentration

After modification of the GP electrode surfaces with the fullerene C_{60} nanomaterial, the electrodes were allowed to incubate with H_2SO_4 solution overnight. Since the fullerene C_{60}

nanomaterial has a very stable and regular structure, this optimization step is very important to expose the carboxyl groups on the GP electrode surface. For this purpose, 4 different concentrations of H_2SO_4 solution (5%, 10%, 25% and 50%) were used to investigate the effect of acid concentration on the proposed biosensor. The biosensors were prepared using each indicated acid concentration and EIS and CV measurements were performed. In this optimization study, it was observed that as the acid concentration increased, the electrode surface was damaged and the immobilization could not be generated correctly. Therefore, lower concentrations were studied. At 5% H_2SO_4 concentration, it was insufficient for surface immobilization. For this reason, optimum H_2SO_4 concentration was determined as 10%. The standard graphs belonging to the optimization study of H_2SO_4 concentration are shown in Fig.S1C.

3.3.3. Optimization studies for ST2 antibody

The next optimization step is to investigate the effect of anti-ST2 concentration on the immunosensor response. The biosensors were prepared using three different concentrations of anti-ST2 solution (2.5 ng mL^{-1}, 5 ng mL^{-1} and 10 ng mL^{-1}) for this optimization step. When the GP electrodes were incubated in 2.5 ng mL^{-1} of anti-ST2 protein, regular EIS signals and a standard calibration graph with a high coefficient of regression were obtained. Then, the concentration of anti-ST2 protein was increased (5 ng mL^{-1}). Thus, it was possible to examine the effect of increased concentrations of the antibody on the proposed immunosensor. By incubation of the electrodes in 5 ng mL^{-1} of anti-ST2 protein, the Rct value indicating the semicircular diameter of the EIS curve was significantly increased (Rct value is 184.1 ohm). When the concentration of anti-ST2 protein was increased further (10 ng mL^{-1}), the performance of the biosensor declined. As is known, when the proteins reach a certain saturation, their activity begins to decline. Considering these reasons, the optimum anti-ST2 concentration for the ST2 immunosensor was chosen as 5 ng mL^{-1} (Fig.S1D).

After determination of the optimum concentration of anti-ST2 protein, studies were carried out to determine the incubation time for anti-ST2 which is another very important parameter. For the immobilization process of the immunosensor, the incubation time of the anti-ST2 solution is important as well as the anti-ST2 concentration used. Since the incubation time has a critical role in influencing protein binding, it is very necessary to determine the optimum time. Therefore, incubation times were also investigated in the scope of optimization studies. Firstly, the electrodes were incubated in anti-ST2 solution for 30 min. In this step, linear but low signals were obtained. This decrease in the signals resulted from the 30 min incubation

period being insufficient for the immobilization of the antibody on the surface. When the electrodes were incubated with anti-ST2 for 60 min, the increase in impedance signals was clearly observed. The increase of impedance signal confirmed that the protein-protein interaction at the electrode surface was successful. Finally, 45 min incubation time was attempted and the results showed the signals again decreased. Thus, the optimum incubation time of anti-ST2 protein was selected as 60 min (Fig.S1E).

3.3.4. Determination of incubation time of ST2 protein

To investigate the effect of incubation times on the proposed immunosensor response, three different times for ST2 incubation (30, 45 and 60 min) were tested. The GP electrodes were incubated in the ST2 solutions for each of these periods. The response of the biosensor was investigated with EIS and CV. As the incubation time for the ST2 protein increased, the activity of ST2 decreased and the EIS signals decreased accordingly. As seen in the results, the incubation time of the ST2 protein to interact with the antibody is optimally 30 min. The signals then reduce due to saturation of the protein on the GP electrode surface. Therefore, the optimum incubation period for ST2 was chosen as 30 min (Fig.S1F).

3.4. Analytical Studies of ST2 immunosensor

The ST2 biomarker was prepared in increasing concentrations and detected with the proposed immunosensor using the EIS and the CV techniques. An excellent linear range was obtained using eight different concentration values for sensitive detection of the ST2 biosensor. The extensive detection range of the proposed immunosensor was determined as a 0.1 fg mL^{-1}– 100 fg mL^{-1}. The calibration curve, the EIS spectrum, and the CV voltammogram of the ST2 immunosensor are presented in Fig.3. However, limit of detection (LOD) and limit of quantification (LOQ) values of the proposed immunosensor were calculated to be 0.124 fg mL^{-1} and 0.414 fg mL^{-1}, respectively. LOD and LOQ values are calculated with the $[k*S_{blank}/m]$ equation which has k as constant (k is accepted as 3 in LOD and as 10 in LOQ), S_{blank} (standard deviation) and m (slope of the calibration curve). Also, the changing impedimetric data with increasing concentrations of ST2 is shown in Fig.3C.

The repeatability study was carried out to clarify the characterization of the developed biosensor. This study was implemented with 20 different disposable GP electrodes which were prepared under the same conditions. The EIS measurement of each electrode was taken using the same concentration value (25 fg mL^{-1}) of the ST2 biomarker. According to these measurements, the average value, standard deviation and coefficient of variation of the

proposed immunosensor were calculated as 25.195 fg mL^{-1}, 0.416 pg mL^{-1}, and 1.56%, respectively.

The reproducibility study of the proposed immunosensor was performed with the GP electrodes prepared in the optimum conditions at different times. For this study, the eight different biosensors were fabricated and their EIS measurements were taken in the detection range of the proposed immunosensor. The relative standard deviations of the proposed immunosensor were calculated as 1.23% (slope) and 7.76% (intercept), respectively. The standard graphs of the study demonstrated that the proposed immunosensor has excellent reproducibility (Fig.3D).

Reusability of a biosensor is a significant property for the surface stability and the cost of the working electrode. Therefore, a regeneration study was carried out to examine the surface stability of the GP electrode. This study was performed with the anti-ST2 modified GP electrode. Firstly, a GP electrode was incubated with ST2 concentration (25 fg mL^{-1}) which is a value on the calibration curve, and the EIS measurement was taken. Then, the GP electrode surface was treated with a HCl acid solution (10 mM, 2 min) to remove ST2 antigen from the surface. This process continued until a high reduction in the ability of the protein to bind to a high extent or its complete loss. The ST2 immunosensor was regenerated with this method 20 times. Moreover, with the 20th binding it was observed to preserve half the activity of the GP electrode. When the difference between 1^{st} binding and 20th binding was examined, total loss of activity was calculated to be 45.77%. This is an excellent reusability performance for a disposable electrode. A promising result was obtained considering the future practical use of the biosensor. The regeneration results of the ST2 biosensor are given in Fig.4A.

Single frequency technique was also utilized for the characterization of the ST2 immunosensor. The investigation of kinetic interactions between anti-ST2 and ST2 antigen is possible thanks to this technique. For this purpose, a constant frequency was determined via the Bode plot in the Gamry Potentiostat/Reference 600. The Bode plot was preferred as it can show the frequency of each point. In accordance with this aim, an impedance measurement at a fixed frequency (45 Hz) was performed as a function of time and phase angle. Fig.4C displays the time dependent changes of impedance in the ST2 biosensor. As seen in Fig.4D, the red curve shows the impedance measurement at fixed frequency and the green curve shows the phase angle. The binding of the ST2 biomarker versus time is clearly seen in this process completed in phosphate buffer (pH 7.0).

The surface coverage study was carried out by using the Laviron equation ($Q=n_xF_xA_x\Gamma$; n: slope, F: Faraday constant (96485 C mol^{-1}), A: Electrode surface area (cm^2), Q: Charge (C) and Γ: Coated surface area (mol cm^{-2})) for the analytical studies of the proposed immunosensor. In order to perform this work, the voltammetric technique was used and the GP electrode surface was scanned at ten different speed values in each immobilization step. These speed values were 10, 20, 30, 40, 50, 60, 70, 80, 90 and 100 mV s^{-1}, respectively. Using the peak currents obtained from the cyclic voltammograms, the calculated data were substituted in the Laviron equation and the surface area of the GP electrode was calculated. When the results were evaluated, the GP surface was initially calculated as $2.2x10^{-8}$ mol cm^{-2}, and was calculated to be $7.3x10^{-8}$ mol cm^{-2} after anti-ST2 binding. This result indicates that anti-ST2 was immobilized onto the surface.

The storage life of an immunosensor is an important parameter for clinical applications. Therefore, the storage life of the ST2 immunosensor was investigated over ten weeks. For this study, ten different GP electrodes were prepared in the same conditions and were kept at +4 ℃ until use. The EIS measurement was taken by incubating with same concentration value of the ST2 protein (25 fg mL^{-1}) every week. In the result of this study, the total activity loss of the biosensor was calculated to be 4.48% at the end of the 10th week (Fig.4B). The storage life of the constructed immunosensor is considered to be suitable for use in clinical applications.

The selectivity study for target ST2 carried out for the constructed immunosensor to understand either there is non-specific interactions or interferences. For this purpose, two GP electrodes were prepared under optimum conditions for the constructed immunosensor. The first electrode was only treated with ST2 solution (50 fg/mL). The other electrode was treated with the solution including ST2 solution (50 fg/mL), cysteine solution (0.2 M), heat shock protein 70 solution (40 fg/mL), protein activated kinase 2 (50 fg/mL), tumor necrosis factor α solution (25 fg/mL), creatine kinase (10 fg/mL). The obtained ΔRct values from the immunosensor responses were compared with each other the results are seen in Fig.3S. The figure proved the proposed immunosensor that has a high selectivity capacity for target ST2.

3.6. Detection of ST2 in Human Serum Samples

In order to examine the usability of the proposed immunosensor for clinical applications, the ST2 biomarker was detected by using the standard addition method with human serum samples obtained from five different individuals. The EIS data were obtained by adding different concentration values of the ST2 protein (5 fg mL^{-1} and 50 fg mL^{-1}) to the serum samples. For this data, the relative standard deviation (RSD) and recovery results were calculated for each serum using the equation from the calibration graph (Table 2).

4. Conclusion

This study presents the fabrication of a reusable, very sensitive and excellent reproducible ST2 immunosensor with a single-use, low-cost, applicable GP electrodes. ST2 is a significant potential biomarker for the early detection of cardiovascular diseases. Moreover, the ST2 antigen was not utilized previously in biosensor applications and is employed as a biodetection element in the literature for the first time in this study. The developed immunosensor was fabricated with a practical immobilization method by using the fullerene C_{60} material which has mechanical strength. All immobilization and optimization studies were characterized with EIS and CV which are strong techniques for electrochemical analyses. However, the morphological characterization of the constructed immunosensor was examined by using the SEM and AFM techniques. The developed immunosensor provided excellent performance in the analysis of other electrochemical techniques (SWV and SFI). Also, the ST2 biosensor had a wide detection range (0.1 fg mL^{-1}– 100 fg mL^{-1}), low LOD (0.124 fg mL^{-1}) and LOQ (0.414 fg mL^{-1}) values. The proposed biosensor exhibited a practical method for ST2 antigen detection with the quite good storage life and stability of the surface. The developed immunosensor could be utilized to detect the ST2 antigen in real human serum samples. More importantly, this immunosensor can detect the ST2 antigen with a drop of human serum. The developed immunosensor can perform the analysis of the ST2 biomarker in the level of sub-femtogram and over a wide detection range. This proposed immunosensor was designed in accordance with the sensitive detection of ST2 which is a potential cardiac biomarker for use in clinical applications.

References

[1] Iwahana, H., Yanagisawa, K., Ito-Kosaka, A., Kuroiwa, K., Tago, K., Komatsu, N.,. Different promoter usage and multiple transcription initiation sites of the interleukin-1 receptor-related human ST2 gene in UT-7 and TM12 cells. Eur. J. Biochem. 264 (1999) 397-406.

[2] Bergers, G., Reikerstorfer, A., Braselmann, S., Graninger, P., Busslinger, M., Alternative promoter usage of the Fos-responsive gene Fit-1 generates mRNA isoforms coding for either secreted or membrane-bound proteins related to the IL-1 receptor. EMBO J. 13 (1994) 1176-88.

[3] Schmitz, J., Owyang, A., Oldham, E., Song, Y., Murphy, E., McClanahan, T. K., IL-33, an interleukin-1-like cytokine that signals via the IL-1 receptor-related protein ST2 and induces T helper type 2-associated cytokines. Immunity. 23 (2005) 479-90.

[4] Sanada, S., Hakuno, D., Higgins, L. J., Schreiter, E. R., McKenzie, A. N., Lee, R. T., IL-33 and ST2 comprise a critical biomechanically induced and cardioprotective signaling system. J. Clin. Invest. 117 (2007) 1538-49.

[5] Stone, R. Search for sepsis drugs goes on despite past failures. Science. 264 (1994) 365- 367.

[6] Hotchkiss, R. S., Swanson, P. E., Freeman, B. D., Tinsley, K. W., Cobb, J. P., Matuschak, G. M., Buchman, T. G., Karl, I. E.,. Apoptotic cell death in patients with sepsis, shock, and multiple organ dysfunction. Crit. Care Med. 27 (1999) 1230-1251.

[7] Ferguson, N. R., Galley, H. F., Webster, N. R., T helper cell subset ratios in patients with severe sepsis. Intensive Care Med. 25 (1999) 106-109.

[8] Roth, G., Moser, B., Krenn, C., Brunner, M., Haisjackl, M., Gerlitz, S., Wolner, E., Boltz-Nitulescu, G., Ankersmit, H. J.,. Susceptibility to programmed cell death in T-lymphocytes from septic patients: a mechanism for lymphopenia and Th2 predominance. Biochem. Biophys. Res. Commun. 308, (2003) 840-846.

[9] Tominaga S. A putative protein of a growth specific cDNA from BALB/c-3T3 cells is highly similar to the extracellular portion of mouse interleukin 1 receptor. *FEBS Lett*. 258 (1989) 301–304.

[10] Yanagisawa, K., Takagi, T., Tsukamoto, T., Identification of the product of the murine ST2 gene. *FEBS Lett*. 318 (1993) 83–87.

[11] Tominaga, S., Kuroiwa, K., Tago, K., Iwahana, H., Yanagisawa, K., Komatsu, N., Presence and expression of a novel variant form of ST2 gene product in human leukemic cell line UT-7/GM. Biochem. Biophys. Res. Commun. 264 (1999) 14-18.

[12] Tominaga, S., Inazawa, J., Tsuji, S., Assignment of the human ST2 gene to chromosome 2 at q11.2. Hum. Genet. 97 (1996) 561-3.

[13] Moritz, D. R., Rodewald, H. R., Gheyselinck, J., Klemenz, R., The IL-1 Receptor-Related T1 Antigen Is Expressed on Immature and Mature Mast Cells and on Fetal Blood Mast Cell Progenitors J. Immunol. 161 (1998) 4866-4874.

[14] Dale, M., Nicklin, M. J., Interleukin-1 receptor cluster: gene organization of IL1R2, IL1R1, IL1RL2 (IL-1Rrp2), IL1RL1 (T1/ST2), and IL18R1 (IL-1Rrp) on human chromosome 2q. Genomics. 57 (1999) 177-179.

[15] Lohning, M., Stroehmann, A., Coyle, A. J., Grogan, J. L., Lin, S., Gutierrez-Ramos, J. C., Levinson, D., Radbruch, A., Kamradt, T., T1/ST2 is preferentially expressed on murine Th2 cells, independent of interleukin 4, interleukin 5, and interleukin 10, and important for Th2 effector function. Proc. Natl. Acad. Sci. USA. 95 (1998) 6930-6935.

[16] Yanagisawa, K., Naito, Y., Kuroiwa, K., Arai, T., Furukawa, Y., Tomizuka, H., Miura, Y., Kasahara, T., Tetsuka, T., Tominaga, S., The expression of ST2 gene in helper T cells and the binding of ST2 protein to myeloma-derived RPMI8226 cells. J. Biochem. 121 (1997) 95-103.

[17] Xu, D., Chan, W. L., Leung, P. B., Huang, F., Wheeler, R., Piedrafita, Robinson, J. H., Liew, F. Y.,. Selective expression of a stable cell surface molecule on type 2 but not type 1 helper T cells. J. Exp. Med. 187 (1998) 787-794.

[18] Tajima, S., Oshikawa, K., Tominaga, S. I., Sugiyama, Y., The Increase in Serum Soluble ST2 Protein Upon Acute Exacerbation of Idiopathic Pulmonary Fibrosis. Chest. 124 (2003) 1206-1214.

[19] Kuroiwa, K., Arai, T., Okazaki, H., Identification of human ST2 protein in the sera of patients with autoimmune diseases. *Biochem Biophys Res. Commun*. 284 (2001) 1104–1108.

[20] Mueller T., Jaffe A. S., Soluble ST2-Analytical Considerations. Am J Cardiol. 115 (2015) 8B-21B

[21] Weinberg E. O., Shimpo M., Hurwitz S., Tominaga S., Rouleau J-L., Lee R. T. Identification of serum soluble ST2 receptor as a novel heart failure biomarker. Clinical Trial. 107 (5) (2003) 721-6.

[22] Aleksova A., Paldino A., Beltrami A. P., Cardiac biomarkers in the emergency department: the role of soluble ST2 (sST2) in acute heart failure and acute coronary syndrome-there is meat on the bone. J. Clin. Med. 8 (2019) 270.

[23] Aurora L., Peterson E., Gui H., Zeld N., McCord J., Pinto Y., Cook B., Sabbah H. N., Williams L. K., Snider J., Lanfear D. E., Suppression Tumorigenicity 2 (ST2) turbidimetric immunoassay compared to enzyme-linked immünosorbent assay in predicting survival in heart failure patients with reduced ejection fraction. Clinica Chimica Acta. 510 (2020) 767-771.

[24] Özkan, S., Bakirhan N. K., Özçelikay G.,. Recent progress on the sensitive detection of cardiovascular disease markers by electrochemical-based biosensors. J. of Phar. and Biomed. Anal. 159 (2018) 406-424.

[25] Pagidipati, N.J., Gaziano, T.A., Estimating Deaths From Cardiovascular Disease: A Review of Global Methodologies of Mortality Measurement. Circulation. 127 (2013) 749–756.

[26] Altintas, Z., Fakanya, W.M., Tothill, I.E., Cardiovascular disease detection using bio-sensing techniques. Talanta. 128 (2014) 177–186.

[27] Yao, Ch., Zhang H.M., Liu T., Li X.F., Liu Z.H., J. Power Sources (2012) 218-455.

[28] Kim J.R., Jung S.H., Regan J.M., Logan B.E.,. Electricity generation and microbial community analysis of alcohol powered microbial fuel cells. Bioresource Technol. 98 (2007) 2568.

[29] Wang, D.W., Li, F., Zhao, J.P., Ren, W.C., Chen, Z.G., Tan, J., Wu, Z.S., Gentle, I., Lu, G.Q., Cheng, H.M. Fabrication of Graphene/Polyaniline Composite Paper via In Situ Anodic Electropolymerization for High-Performance Flexible Electrode. ACS Nano. 3 (2009) 1745.

[30] Cai, W.H., Lai, T., Du, H.J., Ye, J.S.,. Electrochemical determination of ascorbic acid, dopamine and uric acid based on an exfoliated graphite paper electrode: a high performance flexible sensor. Sens. Actuators B. 193 (2014) 492.

[31] Xing, M., Wang, R., Yu, Jianlin., Application of fullerene C60 nano-oil for performance enhancement of domestic refrigerator compressors. International Journal of Refrigeration. 40 (2014) 398-403.

[32] Diederich F. Covalent fullerene chemistry. Pure Appl. Chem. 69 (1997) 395.

[33] Singh, R., Goswami, T.H., Synthesis and evaluation of thermal, photophysical and magnetic properties of novel starlike fullerene–organosilane macromolecules. J. Organomet. Chem. 693 (2008) 2021–2032.

[34] Ravi, P., Dai, S., Hong, K.M., Tam, K.C., Gan, L.H., Self-assembly of C-60 containing poly(methyl methacrylate) in ethyl acetate/decalin mixtures solvent. Polymer 46 (2005) 4714–472.

[35] Demirbakan, B., Sezgintürk M.K.,. A novel immunosensor based on fullerene C60 for electrochemical analysis of heat shock protein 70. J. of. Electroanalytical Chem. 783 (2015) 201-207.

[36] Zhou L., Ting W., Zhang S. Dual-amplified strategy for ultrasensitive electrochemical biosensor based on click chemistry-mediated enzyme-assisted target recycling and functionalized fullerene nanoparticles in the detection of microRNA-141. Biosensors and Bioelectronics 150 (2020) 111964.

[37] Suresh L., Bondili J. S., Brahman P. K. Development of proof of concept for prostate cancer detection: an electrochemical immunosensor based on fullerene-C60 and copper nanoparticles composite film as diagnostic tool. Materials Today Chemistry 16 (2020) 100257.

[38] Anusha T., Bhavani K., S., Brahman P., K. Designing and fabrication of electrochemical nanosensor employing fullerene-C60 and bimetallic nanoparticles composite film for the detection of vitamin D3 in blood samples. Diamond and Related Materials. 104 (2020) 107761.

[39] Ma X., Yuan H., Luan H., Shi Y., Zeng X., Wang Y., Elevated soluble ST2 concentration may involve in the progression of atrial fibrillation. Clinica Chimica Acta. 480 (2018) 138-142.

[40] Chen, L., Huaqing, J.,. A sensitive hydrazine electrochemical sensor based on electrodeposition of gold nanoparticles on choline film modified glassy carbon electrode. Sensors and Actuators B: Chemical. 153 (2011) 239-245.

[41] Sivaraman, N., Dhamodaran, R., Kaliappan, I., Srinivasan, T.G., Rao, P.R.V., Mathews, C.K., Solubility of C60 in organic solvents. J. Org. Chem. 57 (1992) 6077.

[42] Ruoff, R.S., Tse, D.S, Malhotra, Lorents, D.C., Solubility of C_{60} in a variety of solvents. J. Phys. Chem. 97 (1993) 3379.

[43] Wu B.Y., Wang Y.Y., Li J., Song Z., Huang J.D., Wang X.S., Chen Q., An optical biosensor for kinetic analysis of soluble Interleukin-1 receptor I binding to immobilized Interleukin-1alpha. Talanta. 70 (2006) 485-488.

[44] Aldous S.J., Richards A.M., Troughton R., ST2 has diagnostic and prognostic utility for all-cause mortality and heart failure in patients presenting to the emergency department with chest pain. Than M. J Card Fail 18 (2012) 304-310.

[45] Brown A.M., Wu A.H., Clopton P., Robey J.L., Hollander J.E., ST2 in emergency department chest pain patients with potential acute coronary syndromes. Ann Emerg Med 50 (2007) 153-158.

[46] Willems S., Sels J.W., Flier S., Versteeg D., Buhre W.F., de Kleijn D.P., Hoefer I.E., Pasterkamp G. Temporal changes of soluble ST2 after cardiovascular interventions. Eur J Clin Invest. 43 (2012) 113-120.

[47] Wang Y.C., Yu C.C., Chiu F.C., Tsai C.T., Lai L.P., Hwang J.J., Lin J.L., Soluble ST2 as a biomarker for detecting stable heart failure with a normal ejection fraction in hypertensive patients. J Card Fail. 19 (2013) 163-168.

Immobilization Method	Methods	Detection Range	LOD	Reference
CMD cuvette	Optic	100-1600 nM	-	[43]
Critical diagnosis	Marked ST2 kit	‹200 ng mL^{-1}	1.3 ng mL^{-1}	[44]
MBL	Human ELISA ST2 kit	‹20 ng mL^{-1}	0.032 ng mL^{-1}	[45]
Ray-Biotech.	Human IL-1 R4/ST2 ELISA Kit	‹1.2 ng mL^{-}	0.002 ng mL^{-1}	[46]
R&D Systems	IL-1 R4/ST2 ELISA Kit	‹2.0 ng mL^{-1}	0.005 ng mL^{-1}	[47]
GP/Fullerene C_{60}	EIS and CV	0.1 – 100 fg mL^{-1}	0.124 fg mL^{-1}	

Table 1. Comparison of immunological properties of various ST2 immunosensors reported in the literature

Serum Number	ST2 Concentration Value (fg/mL)	Standard Addition Value (fg/mL)	Measurement Conc. Value (fg/mL)	RSD (%) (n=3)	Recovery (%)
1	22.10	5	28.93/30.51/28.88	3.15	108.63
		50	74.08/72.39/73.41	1.16	101.8
2	2.97	5	8.6/8.3/9.7	8.31	111.16
		50	54.03/53.84/52.01	15.59	100.6
3	1.09	5	7.7/6.3/6.73	10.37	113.46
		50	51.2/54.7/54.1	3.5	104.38
4	20.06	5	25.72/26.92/26.5	2.3	105.26
		50	72.13/69.47/71.17	1.9	101.22
5	16.31	5	23.08/22.58/23.06	1.24	107.46
		50	68.41/64.90/65.63	2.79	100.00

Table.2. Analysis of ST2 biosensor in real serum samples by standard addition method.

Figures

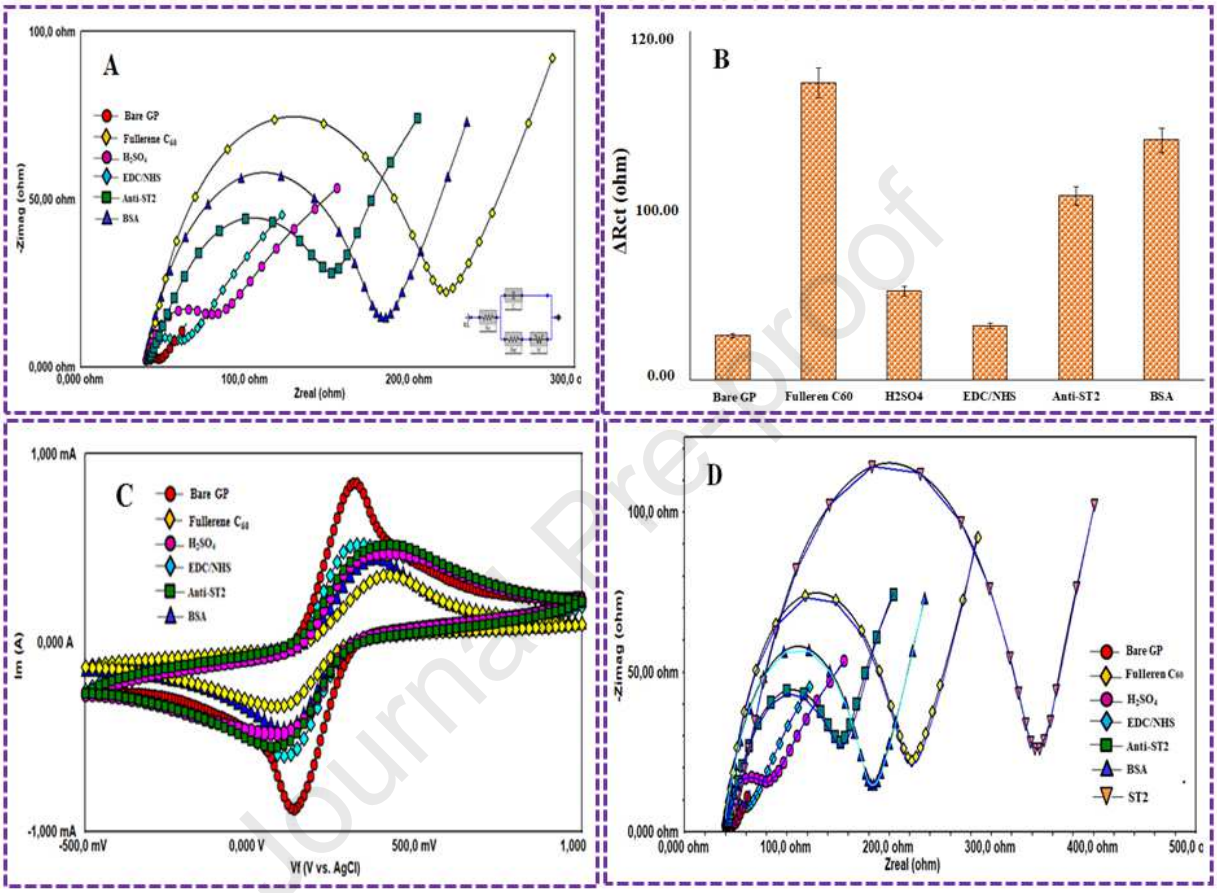

Figure 1. EIS spectra (A), Rct values (B) CV voltammograms (C) of the ST2 immunosensor and Kramer's Kronig Tranform (D).

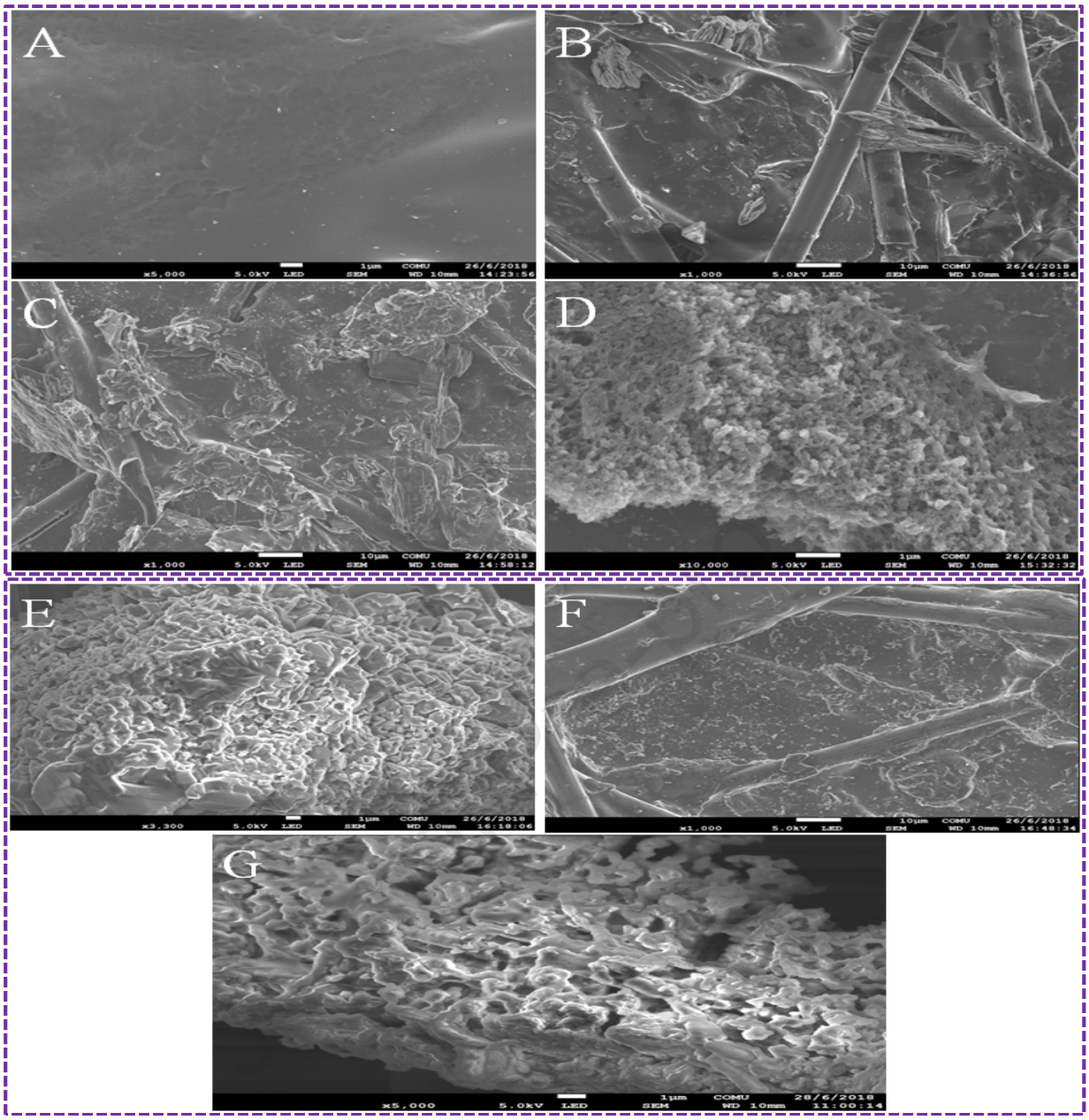
A
B
C
D
E
F
G

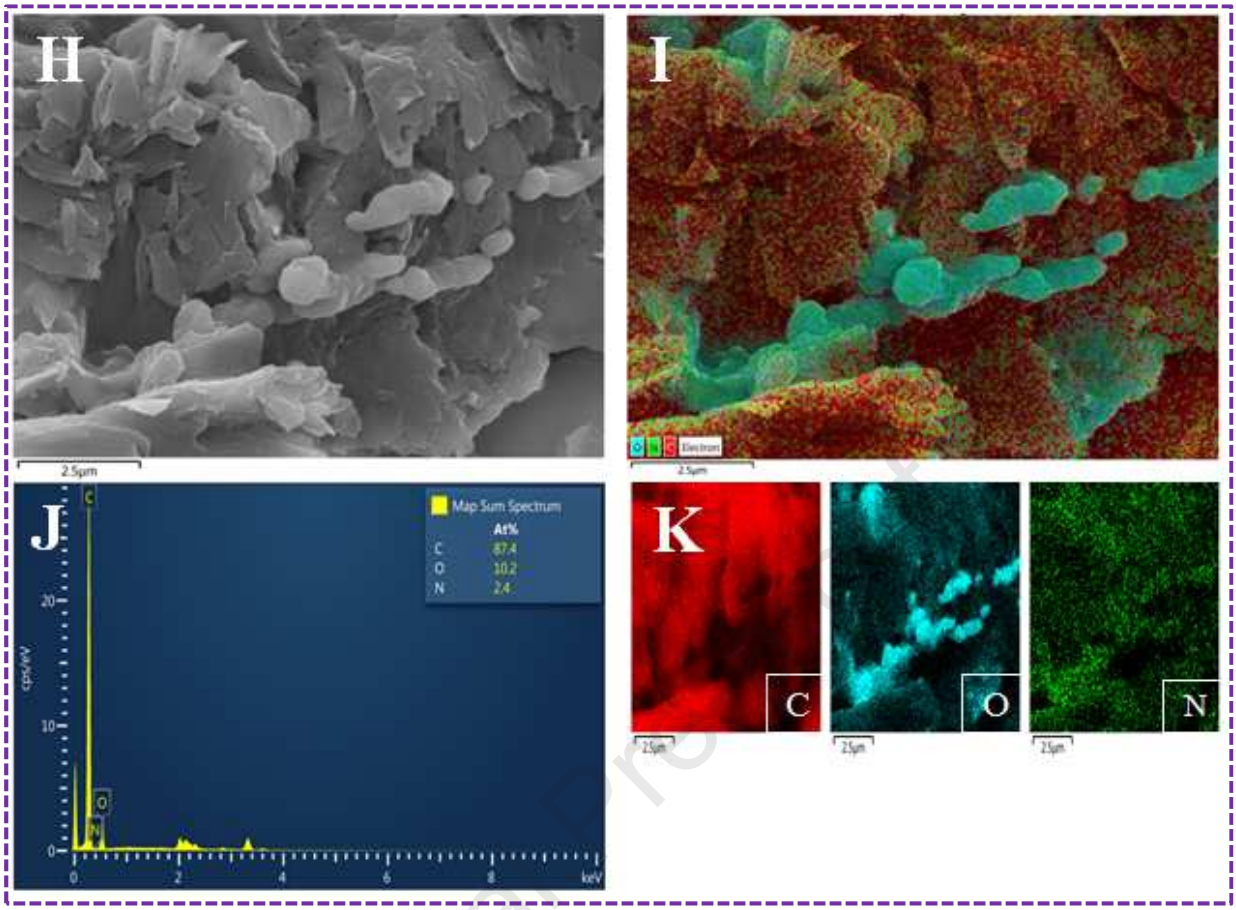

Figure 2. SEM images of bare GP electrode (A), Fullerene C_{60} modified GP electrode (B), after H_2SO_4 incubation GP electrode (C), after EDC/NHS incubation GP electrode (D), after anti-ST2 immobilization GP electrode (E), BSA blockage (F), after ST2 antigen immobilization GP electrode (G). SEM image (H), Mapping (I), (J) EDX spectrum (K) of the ST2 antigen on the GP surface.

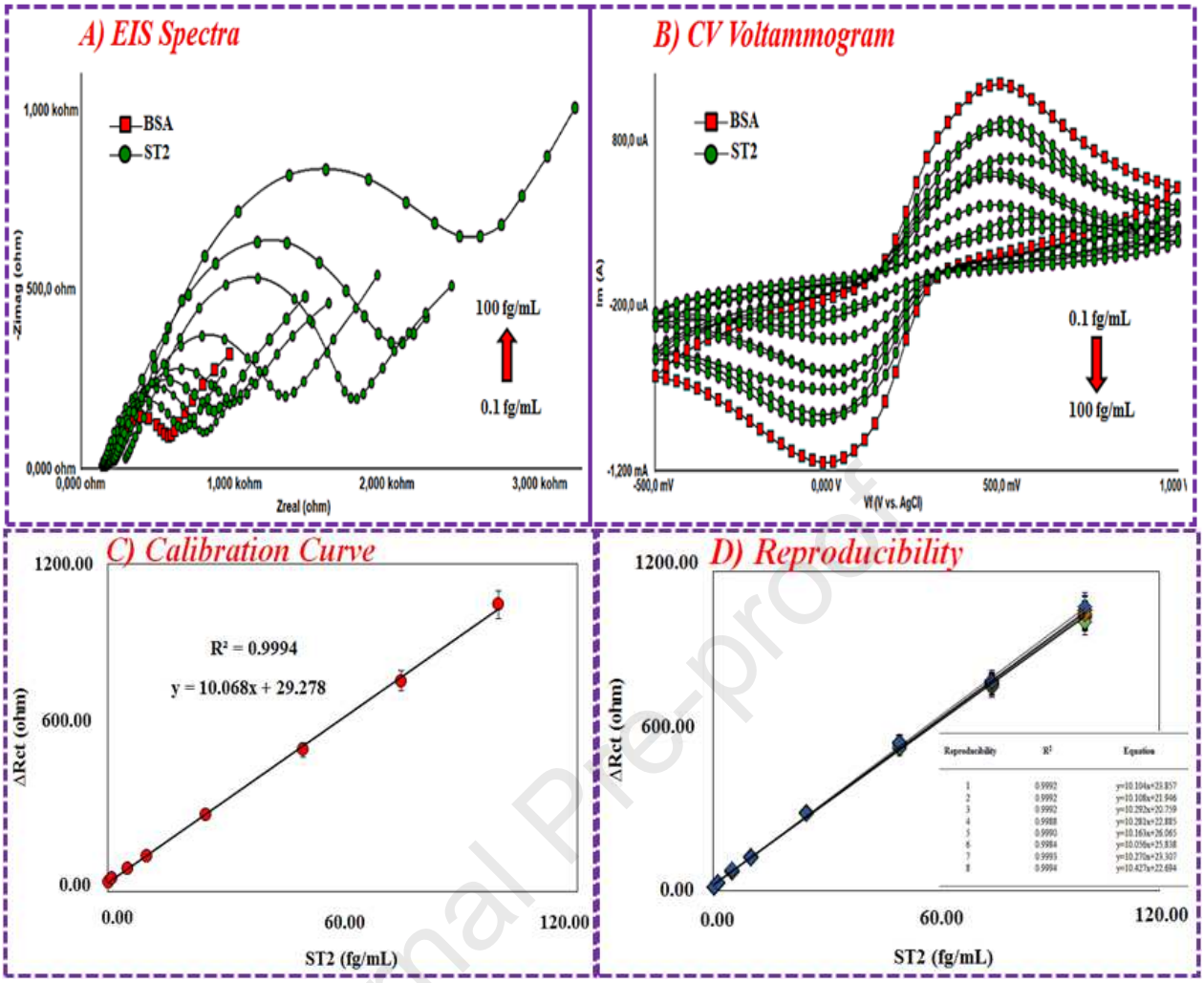

Figure 3. (A) EIS spectra, (B) CV voltammograms of the detection of the ST2 at increased concentrations, (C) Calibration curve of the ST2 biosensor, (D) Reproducibility,

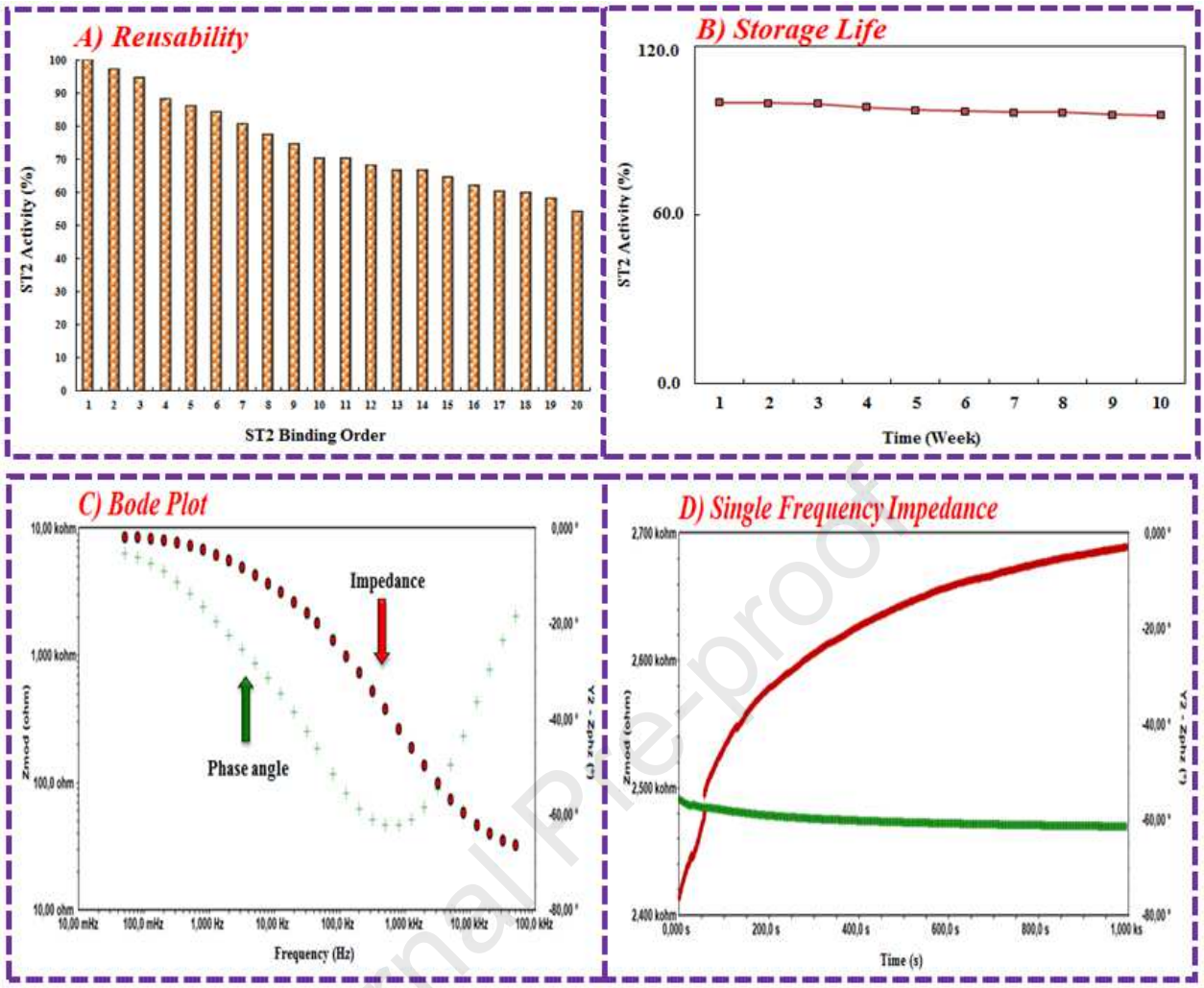

Figure 4. (A) Reusability, (B) Storage Life, (C) Bode plot for SFI analysis, (D) Impedance measurement in the SFI analysis

Immobilization Method	Methods	Detection Range	LOD	Reference
CMD cuvette	Optic	100-1600 nM	-	[43]
Critical diagnosis	Marked ST2 kit	‹200 ng mL^{-1}	1.3 ng mL^{-1}	[44]
MBL	Human ELISA ST2 kit	‹20 ng mL^{-1}	0.032 ng mL^{-1}	[45]
Ray-Biotech.	Human IL-1 R4/ST2 ELISA Kit	‹1.2 ng mL^{-}	0.002 ng mL^{-1}	[46]
R&D Systems	IL-1 R4/ST2 ELISA Kit	‹2.0 ng mL^{-1}	0.005 ng mL^{-1}	[47]
GP/Fullerene C_{60}	EIS and CV	0.1 – 100 fg mL^{-1}	0.124 fg mL^{-1}	

Table 1. Comparison of immunological properties of various ST2 immunosensors reported in the literature

Serum Number	ST2 Concentration Value (fg/mL)	Standard Addition Value (fg/mL)	Measurement Conc. Value (fg/mL)	RSD (%) (n=3)	Recovery (%)
1	22.10	5	28.93/30.51/28.88	3.15	108.63
		50	74.08/72.39/73.41	1.16	101.8
2	2.97	5	8.6/8.3/9.7	8.31	111.16
		50	54.03/53.84/52.01	15.59	100.6
3	1.09	5	7.7/6.3/6.73	10.37	113.46
		50	51.2/54.7/54.1	3.5	104.38
4	20.06	5	25.72/26.92/26.5	2.3	105.26
		50	72.13/69.47/71.17	1.9	101.22
5	16.31	5	23.08/22.58/23.06	1.24	107.46
		50	68.41/64.90/65.63	2.79	100.00

Table.2. Analysis of ST2 biosensor in real serum samples by standard addition method.

Highlights

The electrochemical immunosensor designed a practical, low-cost and sensitive method for determination of Suppression of Tumorigenicity 2.

ST2 immunosensor exhibited high analytical performance with a linear range 0.1 fg/mL – 100 fg/mL and low detection limit (1.28 fg/mL).

Single-use graphite paper electrodes were firstly used to detection ST2 antigen for a novel biosensor system.

The optimization was performed for all fabrication steps of the electrochemical biosensor system.

Declaration of interests

☒ The authors declare that they have no known competing financial interests or personal relationships that could have appeared to influence the work reported in this paper.

☐The authors declare the following financial interests/personal relationships which may be considered as potential competing interests: